*Inorg. Chem.* **2002**, *41*, 2864–2870

# Structural Basis for Unusually Long Wavelength Charge Transfer Transitions in Complexes [MCl(ECH$_2$CH$_2$NMe$_2$)(PR$_3$)] (E = Te, Se; M = Pt, Pd): Experimental Results and TD-DFT Calculations

**Sandip Dey,[†] Vimal K. Jain,*[,†] Axel Knödler,[‡] Axel Klein,[‡] Wolfgang Kaim,*[,‡] and Stanislav Záliš[§]**

*Novel Materials and Structural Chemistry Division, Bhabha Atomic Research Centre, Trombay, Mumbai 400085, India, Institut für Anorganische Chemie, Universität Stuttgart, Pfaffenwaldring 55, D-70550 Stuttgart, Germany, and J. Heyrovsky Institute of Physical Chemistry, Academy of Sciences of the Czech Republic, Dolejškova 3, CZ-18223 Prague, Czech Republic*

Received November 28, 2001

A series of new complexes, the blue compounds [PdCl(TeCH$_2$CH$_2$NMe$_2$)(PR$_3$)] (PR$_3$ = PEt$_3$, PPr$^n_3$, PBu$^n_3$, PMe$_2$Ph, PMePh$_2$, PPh$_3$, PTol$_3$) and the red [PtCl(TeCH$_2$CH$_2$NMe$_2$)(PR$_3$)] (PR$_3$ = PMe$_2$Ph, PMePh$_2$), were synthesized and studied spectroscopically ($^1$H and $^{31}$P NMR, UV/vis) and by cyclic voltammetry. The structures of [PdCl(TeCH$_2$CH$_2$NMe$_2$)(PPr$^n_3$)] (**2b**) [PdCl(TeCH$_2$CH$_2$NMe$_2$)(PMePh$_2$)] (**2e**), [PtCl(TeCH$_2$CH$_2$NMe$_2$)(PMePh$_2$)] (**2i**), and the related [PtCl(SeCH$_2$CH$_2$NMe$_2$)(PEt$_3$)] (**3**) were determined crystallographically, revealing a typical pattern of trans-positioned neutral N and P donor atoms in an approximately square planar setting. The molecules **2b**, **2e**, and **2i** were calculated by TD-DFT methodology to understand the origin of the weak ($\epsilon \approx 200$ M$^{-1}$ cm$^{-1}$) long-wavelength bands at about 600 nm for Pd/Te complexes such as **2b** or **2e**, at ca. 460 nm for Pt/Te systems such as **2i**, and at about 405 nm for Pt/Se analogues such as **3**. These transitions are identified as charge transfer transitions from the selenolato or tellurolato centers to unoccupied orbitals involving mainly the phosphine coligands for the Pt$^{II}$ compounds and more delocalized MOs for the Pd$^{II}$ analogues. Calculations and electrochemical data were used to rationalize the effects of metal and chalcogen variation.

## Introduction

Metal-mediated interaction between coordinated ligands is an important aspect of coordination chemistry. As an example, the charge transfer interactions between metal-bound donor and acceptor centers have been recognized and described qualitatively in planar complexes of group 10 metals with thiolato donors and α-diimine acceptors.[1,2a−c] The possible function of organophosphines as acceptor components for charge transfer transitions in complexes has been reviewed recently.[2d] In this work we present a study which involves Pd$^{II}$- or Pt$^{II}$-bound selenolate or tellurolate donors and triorganophosphines as acceptors in complexes [MCl(ECH$_2$CH$_2$NMe$_2$)(PR$_3$)] (E = Se, Te; M = Pd, Pt). This combination of heavier elements for main group donor, acceptor, *and* transition metal mediator poses a formidable challenge for quantum chemical calculations which we sought to interpret the unusual long-wavelength absorptions in a more quantitative way; corresponding methods such as relativistic time-dependent density functional theory (TD-DFT) have only recently become applicable to such large systems containing heavy elements.[3]

Based on the crystallographically determined structures of compounds [PdCl(TeCH$_2$CH$_2$NMe$_2$)(PPr$^n_3$)] (**2b**), [PdCl(TeCH$_2$CH$_2$NMe$_2$)(PMePh$_2$)] (**2e**), and [PtCl(TeCH$_2$CH$_2$NMe$_2$)(PMePh$_2$)] (**2i**) we present TD-DFT calculations and electrochemical measurements to understand the conspicuous

* Authors to whom correspondence should be addressed. E-mail: kaim@iac.uni-stuttgart.de (W.K.); jainvk@apsara.barc.ernet.in (V.K.J.).
† Bhabha Atomic Research Centre.
‡ Universität Stuttgart.
§ Heyrovsky Institute.

(1) (a) Paw, W.; Lachicotte, R. J.; Eisenberg, R. *Inorg. Chem.* **1998**, *37*, 4139. (b) Cummings, S. D.; Eisenberg, R. *J. Am. Chem. Soc.* **1996**, *118*, 1949. (c) Connick, W. B.; Gray, H. B. *J. Am. Chem. Soc.* **1997**, *119*, 11620.
(2) (a) Vogler, A.; Kunkely, H. *Top. Curr. Chem.* **1990**, *158*, 1. (b) Kunkely, H.; Vogler, A. *J. Organomet. Chem.* **1993**, *453*, 269. (c) Kunkely, H.; Vogler, A. *Inorg. Chim. Acta* **1997**, *264*, 305. (d) Vogler, A.; Kunkely, H. *Coord. Chem. Rev.*, in press.
(3) Rosa, A.; Baerends, E. J.; van Gisbergen, S. J. A.; van Lenthe, E.; Groeneveld, J. A.; Snijders, J. G. *J. Am. Chem. Soc.* **1999**, *121*, 10356.



10.1021/ic011210v CCC: $22.00 
Published on Web 05/07/2002

colors of the complexes. The comparison with corresponding selenolato systems[4a] such as the now structurally characterized [PtCl($SeCH_2CH_2NMe_2$)($PEt_3$)] (**3**) serves to further elucidate the electronic structures of these compounds.

## Experimental Section

**Materials and Instrumentation.** All syntheses were carried out under high-purity nitrogen in dry and distilled analytical grade solvents. Tellurium (99.99%), tertiary phosphines (Strem Chemicals), and $Me_2NCH_2CH_2Cl$·HCl were obtained from commercial sources. The complexes $Na_2PdCl_4$, [$M_2Cl_2(\mu\text{-}Cl)_2(PR_3)_2$] ($PR_3$ = $PEt_3$, $PPr^n_3$, $PBu^n_3$, $PMe_2Ph$, $PMePh_2$, $PPh_3$, or $PTol_3$, Tol = *p*-tolyl),[4b] and [PtCl($SeCH_2CH_2NMe_2$)($PEt_3$)] (**3**) were prepared according to literature methods. Melting points were determined in capillary tubes and are uncorrected. Elemental analyses were carried out by the Analytical Chemistry Division of BARC. $^1$H, $^{13}$C{$^1$H}, and $^{31}$P{$^1$H} NMR spectra were recorded on a Bruker DPX-300 NMR spectrometer operating at 300, 75.47, and 121.49 MHz, respectively. Chemical shifts are relative to internal solvent peaks for $^1$H and $^{13}$C NMR resonances and to external 85% $H_3PO_4$ for $^{31}$P NMR signals. UV/vis absorption spectra were recorded in $CH_2Cl_2$ on a Bruins Instruments Omega 10 spectrophotometer. Cyclic voltammetry was carried at a 100 mV/s scan rate in dichloromethane/0.1 M $Bu_4NPF_6$ using a three-electrode configuration (glassy carbon working electrode, Pt counter electrode, Ag/AgCl reference) and a PAR 273 potentiostat and function generator. The ferrocene/ferrocenium couple served as internal reference.

All spectroscopic data of compounds **2a**−**i** were obtained for freshly prepared solutions; the colors of the solutions change (within ca. 1 h for palladium complexes) when left at room temperature. This behavior of tellurolate complexes of Pd or Pt is not uncommon.[5]

**Syntheses. ($Me_2NCH_2CH_2Te)_2$.** Bis(2-dimethylaminoethyl)ditelluride was prepared via the general method reported by Li et al.,[6] involving the reduction of Te powder with $PhNHNH_2$ in DMF, followed by treatment with $Me_2NCH_2CH_2Cl$. The red, air- and moisture-sensitive liquid was distilled in vacuo (110−118 °C, 0.01 mmHg). $^1$H NMR ($CDCl_3$): $\delta$ 2.25 (s, 6H, $NMe_2$); 2.56 (t, 7.4 Hz, 2H, $SeCH_2$) and 3.27 (t, 7.4 Hz, 2H, $NCH_2$).[7] $^{13}$C{$^1$H} NMR ($CDCl_3$): $\delta$ 5.3 (s, $TeCH_2$); 44.9 (s, $NMe_2$); 62.0 (s, $NCH_2$).

**[PdCl($TeCH_2CH_2NMe_2$)]$_n$ (1).** Solid $Na_2PdCl_4$ (1.86 g, 6.32 mmol) was added to a stirred methanolic solution of ($Me_2NCH_2CH_2Te)_2$ (1.26 g, 3.15 mmol) at room temperature, whereupon a brownish yellow solid precipitated. The mixture was stirred for 4 h. The solid was washed with methanol, water, acetone, and diethyl ether and dried in vacuo (yield: 1.51 g, 70%). It was recrystallized from $CH_2Cl_2$ as a brown solid (370 mg, 25%); mp >180 °C dec. Anal. Calcd for $C_4H_{10}ClNPdTe$: C, 14.0; H, 3.0; N, 4.1. Found: C, 13.5; H, 2.6; N, 4.5.

**[PdCl($TeCH_2CH_2NMe_2$)($PEt_3$)] (2a).** To a methanolic solution (10 cm$^3$) of $NaTeCH_2CH_2NMe_2$ as prepared from ($Me_2NCH_2CH_2Te)_2$ (194 mg, 0.33 mmol) and $NaBH_4$ (26 mg, 0.68 mmol) was added an acetone suspension (25 cm$^3$) of [$Pd_2Cl_2(\mu\text{-}Cl)_2(PEt_3)_2$] (194 mg, 0.33 mmol); the reaction mixture was then stirred for 3 h at room temperature. The solvents were evaporated in vacuo, and the residue was extracted with hexane (3 × 10 cm$^3$). The extracts were passed through a Florisil column to yield a blue solution, which was concentrated and kept at −4 °C to yield air-sensitive blue crystals in 60% yield (182 mg). The other palladium and platinum complexes **2b**−**i** were prepared in an analogous manner. **2a**: Anal. Calcd for $C_{10}H_{25}ClNPdTe$: C, 26.1; H, 5.5; N, 3.1. Found: C, 25.5; H, 5.2; N, 3.1. $^1$H NMR ($CDCl_3$): $\delta$ 1.16 (td, 17.4 Hz (d), 7.6 Hz (t); $PCH_2$*Me*); 1.83−1.94 (m, $PCH_2$); 2.62 (d, 2.8 Hz, $NMe_2$); 2.80 (t, 6.0 Hz, $TeCH_2$); 3.49 (t, 5.0 Hz, $NCH_2$). $^{31}$P{$^1$H} NMR ($CDCl_3$): $\delta$ 26.6 (s).

**[PdCl($TeCH_2CH_2NMe_2$)($PPr^n_3$)] (2b):** recrystallized from hexane in 70% yield, mp 81 °C. Anal. Calcd for $C_{13}H_3ClNPPdTe$: C, 31.1; H, 6.2; N, 2.8. Found: C, 31.5; H, 6.4; N, 2.7. $^1$H NMR ($CDCl_3$): $\delta$ 1.02 (t, 7.2 Hz, PCC*Me*); 1.53−1.84 (m, $PCH_2CH_2$-); 2.57 (d, 2.8 Hz, $NMe_2$); 2.77 (t, 6.0 Hz, $TeCH_2$); 3.46 (t, 6.0 Hz, $NCH_2$). $^{31}$P{$^1$H} NMR (acetone-$d_6$): $\delta$ 16.7 (s).

**[PdCl($TeCH_2CH_2NMe_2$)($PBu^n_3$)] (2c):** recrystallized from hexane in 74% yield. Anal. Calcd for $C_{16}H_{37}ClNPPdTe$: C, 35.3; H, 6.9; N, 2.6. Found: C, 35.5; H, 7.0; N, 2.5. $^1$H NMR (acetone-$d_6$): $\delta$ 0.93 (t, 7.2 Hz, PCCCMe); 1.41−1.90 (m, $PCH_2CH_2CH_2$-); 2.57 (d, 2.8 Hz, $NMe_2$); 2.78 (t, 3.0 Hz, $TeCH_2$); 3.50 (m, $NCH_2$). $^{31}$P-{$^1$H} NMR (acetone-$d_6$): $\delta$ 18.1 (s).

**[PdCl($TeCH_2CH_2NMe_2$)($PMe_2Ph$)] (2d):** recrystallized from $CH_2Cl_2$−$Me_2CO$ in 65% yield, mp 132 °C. Anal. Calcd for $C_{12}H_{21}$-ClNPPdTe: C, 30.0; H, 4.4; N, 2.9. Found: C, 29.5; H, 3.9; N, 2.6. $^1$H NMR ($CDCl_3$): $\delta$ 1.91 (d, 11.4 Hz, $PMe_2$); 2.62 (d, 2.8 Hz, $NMe_2$); 2.71 (br, $TeCH_2$); 3.61 (t, 5.0 Hz, $NCH_2$); 7.41 (m, Ph), 7.62 (m, Ph). $^{31}$P{$^1$H} NMR ($CDCl_3$): $\delta$ −6.1 (s).

**[PdCl($TeCH_2CH_2NMe_2$)($PMePh_2$)] (2e):** recrystallized from $CH_2Cl_2$−$Me_2CO$ in 58% yield, mp 172 °C. Anal. Calcd for $C_{17}H_{23}$-ClNPPdTe: C, 37.7; H, 4.3; N, 2.6. Found: C, 37.3; H, 4.3; N, 2.4. $^1$H NMR ($CDCl_3$): $\delta$ 2.26 (d, 11.4 Hz, PMe); 2.67 (merged in $NMe_2$ resonance, $TeCH_2$); 2.68 (d, 2.8 Hz, $NMe_2$); 3.73 (t, 5.0 Hz, $NCH_2$); 7.40 (m, Ph), 7.63 (m, Ph). $^{31}$P{$^1$H} NMR ($CDCl_3$): $\delta$ 8.7 (s).

**[PdCl($TeCH_2CH_2NMe_2$)($PPh_3$)] (2f):** (i) recrystallized from $CH_2Cl_2$−$Me_2CO$ in 52% yield, mp 154 °C dec. Anal. Calcd for $C_{22}H_{25}ClNPPdTe$: C, 43.7; H, 4.2; N, 2.3. Found: C, 42.9; H, 4.3; N, 2.1. $^1$H NMR ($CDCl_3$): $\delta$ 2.69 (merged in N*Me*$_2$ protons, $TeCH_2$); 2.74 (d, 2.8 Hz, $NMe_2$); 3.84 (t, 5.0 Hz, $NCH_2$); 7.25−7.35 (m, Ph), 7.80−7.85 (m, Ph). $^{31}$P{$^1$H} NMR: $\delta$ 21.9 (s). (ii) Solid $PPh_3$ (330 mg, 1.26 mmol) was added to an acetone suspension of (30 cm$^3$) of **1** (428 mg, 1.25 mmol), and the mixture was stirred for 3 h under $N_2$. The green solution was filtered, and the filtrate was dried in vacuo to give a greenish yellow solid. The solid was washed with hexane, diethyl ether, and acetone to remove unreacted $PPh_3$ and recrystallized from dichloromethane−acetone (yield 498 mg, 52%). Analytical and spectroscopic data are similar to those of the sample prepared via route i.

**[PdCl($TeCH_2CH_2NMe_2$)($PTol_3$)] (2g):** prepared similarly to **2f**, method ii, and recrystallized from acetone−hexane in 56% yield, mp 108 °C. Anal. Calcd for $C_{25}H_{31}ClNPPdTe$: C, 46.5; H, 4.8; N, 2.2. Found: C, 44.8; H, 5.1; N, 1.7. $^1$H NMR ($CDCl_3$): $\delta$ 2.68 (t, merged with $NMe_2$ protons, $TeCH_2$); 2.72 (d, 2.8 Hz, $NMe_2$); 3.78 (t, 5.0 Hz, $NCH_2$); 7.15 (d, 7.5 Hz, $C_6H_4$), 7.62 (d, 7.5 Hz, $C_6H_4$). $^{31}$P{$^1$H} NMR ($CDCl_3$): $\delta$ 19.8 (s).

**[PtCl($TeCH_2CH_2NMe_2$)($PMe_2Ph$)] (2h):** recrystallized from $CH_2Cl_2$−$Me_2CO$ in 68% yield, mp 148 °C. Anal. Calcd for $C_{12}H_{21}$-ClNPPtTe: C, 25.4; H, 3.7; N, 2.5. Found: C, 25.4; H, 3.7; N, 2.5. $^1$H NMR ($CDCl_3$): $\delta$ 1.92 (d, 11.3 Hz, $^3J$(Pt−H) 34 Hz, $PMe_2$); 2.29 (t, 6.0 Hz, $TeCH_2$); 2.74 (d, 2.8 Hz, with 14.0 Hz $^3J$(Pt−H), $NMe_2$); 3.36 (t, 6.0 Hz, $NCH_2$); 7.38 (m, Ph), 7.67 (m, Ph). $^{31}$P-{$^1$H} NMR ($CDCl_3$): $\delta$ −26.5, $^1J$($^{195}$Pt−$^{31}$P) 3382 Hz.

(4) (a) Dey, S.; Jain, V. K.; Knoedler, A.; Kaim, W.; Zalis, S. *Eur. J. Inorg. Chem*. **2001**, 2965. (b) Dey, S.; Jain, V. K.; Varghese, B. *J. Organomet. Chem.* **2001**, *623*, 48.
(5) (a) Jain, V. K.; Kannan, S. *J. Organomet. Chem.* **1991**, *418*, 349. (b) Kannan, S. Ph.D. Thesis, Mumbai University, 1992.
(6) Li, J. Q.; Bao, W. L.; Lue, P.; Zhou, X. *Synth. Commun.* **1996**, *21*, 799.
(7) Srivastava, V.; Batheja, R.; Singh, A. K. *J. Organomet. Chem.* **1994**, *484*, 93.

**Table 1.** Crystallographic and Structure Refinement Data of Complexes $[MCl(ECH_2CH_2NMe_2)(PR_3)]$

| | M/E/$PR_3$ | | | |
|---|---|---|---|---|
| | Pd/Te/$PPr^n_3$ (**2b**) | Pd/Te/$PMePh_2$ (**2e**) | Pt/Te/$PMePh_2$ (**2i**) | Pt/Se/$PEt_3$ (**3**) |
| chem formula | $C_{13}H_{31}ClNPPdTe$ | $C_{17}H_{23}ClNPPdTe$ | $C_{17}H_{23}ClNPPtTe$ | $C_{10}H_{25}ClNPtSe$ |
| fw | 501.81 | 541.78 | 630.47 | 499.78 |
| cryst size (mm) | 0.5 × 0.3 × 0.3 | 0.3 × 0.3 × 0.2 | 0.1 × 0.1 × 0.05 | 0.1 × 0.1 × 0.3 |
| *T*/K | 173(2) | 173(2) | 293(2) | 173(2) |
| *λ*/Å | 0.71073 | 0.71073 | 0.71073 | 0.71073 |
| cryst syst | triclinic | monoclinic | monoclinic | orthorhombic |
| space group | $P\bar{1}$ | $P2_1/c$ | $P2_1/c$ | $P2_12_12_1$ |
| *a*/Å | 8.413(2) | 11.627(2) | 11.682(2) | 9.6374(19) |
| *b*/Å | 10.709(3) | 13.388(3) | 13.499(3) | 11.5216(16) |
| *c*/Å | 11.406(3) | 11.859(2) | 12.926(3) | 13.917(2) |
| α/deg | 74.096(17) | 90 | 90 | 90 |
| *β*/deg | 85.768(18) | 106.88(3) | 106.70(3) | 90 |
| *γ*/deg | 72.795(19) | 90 | 90 | 90 |
| *V*/Å$^3$ | 944.1(4) | 1766.5(6) | 1952.6(7) | 1545.3(4) |
| $\rho_{calcd}$, g cm$^{-3}$ | 1.765 | 2.037 | 2.145 | 2.148 |
| *Z* | 2 | 4 | 4 | 4 |
| *μ*/mm$^{-1}$ | 2.711 | 2.907 | 8.866 | 11.687 |
| reflns collected/unique | 5536/4663 | 4974/4476 | 13907/1968 | 3801/3293 |
| data/restraints/params | 4663/0/163 | 4476/0/200 | 1968/0/200 | 3293/0/136 |
| final R1, wR2 indices | 0.0332, 0.0799 | 0.0425, 0.1076 | 0.0301, 0.0768 | 0.0424, 0.0986 |
| R1, wR2 (all data) | 0.0430, 0.0850 | 0.0561, 0.1147 | 0.0319, 0.0788 | 0.0557, 0.1064 |

**$[PtCl(TeCH_2CH_2NMe_2)(PMePh_2)]$ (2i):** recrystallized from acetone−hexane in 64% yield, mp 166 °C dec. Anal. Calcd for $C_{17}H_{23}ClNPPtTe$: C, 32.4; H, 3.7; N, 2.2. Found: C, 32.2; H, 3.7; N, 2.1. $^1$H NMR ($CDCl_3$): $\delta$ 2.28 (d, 11.2 Hz, $^3J$(Pt−H) = 32 Hz, $PMe_2$); 2.80 ($TeCH_2$ merged in $NMe_2$ resonance); 2.80 (d, 2.8 Hz, $^3J$(Pt−H) = 18 Hz, $NMe_2$); 3.48 (t, 6.0 Hz, $NCH_2$); 7.39 (m, Ph), 7.58−7.66 (m, Ph). $^{31}$P{$^1$H} NMR ($CDCl_3$): $\delta$ −11.1, $^1J$($^{195}$Pt−$^{31}$P) 3491 Hz.

**Crystallography.** Single crystals of $[PdCl(TeCH_2CH_2NMe_2)(PMePh_2)]$ (**2e**) and $[PtCl(TeCH_2CH_2NMe_2)(PMePh_2)]$ (**2i**) were obtained at −10 °C from $CH_2Cl_2$−acetone and acetone−hexane mixtures, respectively, while single crystals of $[PdCl(TeCH_2CH_2NMe_2)(PPr^n_3)]$ (**2b**) and $[PtCl(SeCH_2CH_2NMe_2)(PEt_3)]$ (**3**) were obtained from concentrated hexane solutions. X-ray data of **3**,[4a] of a purple-pink crystal of **2b**, and of a blue crystal of **2e** were collected at 173(2) K on Siemens P4 and P3 diffractometers, using graphite-monochromated Mo Kα radiation ($\lambda$ = 0.71073 Å) and employing the $\omega-2\theta$ scan technique. X-ray data of a red crystal of **2i** were collected on a Nonius Kappa CCD diffractometer at room temperature. The unit cell parameters (Table 1) were determined from 25 reflections measured by a random search routine. The intensity data were measured for Lorentz polarization and absorption effects ($\psi$ scans). The structures of **2b**, **2i**, and **3** were solved by the Patterson method while the structure of **2e** was solved by direct methods (program SHELXTL 5.1[8]). The non-hydrogen atoms were refined anisotropically, and the hydrogen atoms were introduced (riding model).

**DFT Calculations.** Ground state electronic structure calculations on complexes $[MCl(TeCH_2CH_2NMe_2)(PR_3)]$ (M = Pd, Pt, $PR_3$ = $PPr^n_3$, $PMe_2Ph$, $PMePh_2$) have been done by density-functional theory (DFT) methods using the ADF2000.02[9,10] program package. The lowest excited states of the closed-shell complexes were calculated by the time-dependent DFT (TD-DFT) method.

Within the ADF program, Slater type orbital (STO) basis sets of double-ζ quality with polarization functions within methyl, propyl, and phenyl substituent groups and triple-ζ quality for the rest of the system were employed. The inner shells were represented by the frozen core approximation (1s for C, N, 1s-2p for P and Cl, 1s-4p for Te, 1s-3d for Pd, and 1s-4d for Pt were kept frozen). The following density functionals were used within ADF: the local density approximation (LDA) with VWN parametrization of electron gas data or the functional including Becke's gradient correction[11] to the local exchange expression in conjunction with Perdew's gradient correction[12] to the LDA expression (ADF/BP). The scalar relativistic (SR) zero order regular approximation (ZORA) was used within this study. The TD-DFT calculations were done using the optimized geometries of the $[MCl(TeCH_2CH_2NMe_2)(L)]$ complexes.

## Results and Discussion

**Synthesis and NMR Spectroscopy.** When $Na_2PdCl_4$ was treated with a methanolic solution of $(Me_2NCH_2CH_2Te)_2$, a brown insoluble product of the composition $[PdCl(TeCH_2CH_2NMe_2)]_n$ (**1**) was isolated. The analogous selenolate $[PdCl(SeCH_2CH_2NMe_2)]_n$ exists as a structurally characterized trimeric molecule ($n$ = 3).[13] When **1** was treated with tertiary phosphines, complexes of the general formula $[PdCl(TeCH_2CH_2NMe_2)(PR_3)]$ (**2**) were isolated. Compounds **2a**−**i** are also readily prepared by reacting $[Pd_2Cl_2(\mu\text{-}Cl)_2(PR_3)_2]$ with $NaTeCH_2CH_2NMe_2$ in a 1:2 molar ratio. This reaction can be extended for the preaparation of platinum analogues (Scheme 1).

The $^1$H NMR spectra of **2** show characteristic resonances. The $NMe_2$ signal appears as a doublet due to $^4J$(Pt−H) coupling. The resonances for the platinum complexes are flanked by $^{195}$Pt satellites with the $^3J$(Pt−H) values comparable to those of the corresponding selenolate complexes.[4a] The $^{31}$P NMR spectra exhibit single resonances indicating the formation of only one isomer. The magnitude of $^1J$(Pt−

(8) *SHELXTL 5.1*; Bruker Analytical X-Ray Systems: Madison, WI, 1998.
(9) Fonseca Guerra, C.; Snijders, J. G.; Te Velde, G.; Baerends, E. J. *Theor. Chem. Acc.* **1998**, *99*, 391.
(10) van Gisbergen, S. J. A.; Snijders, J. G.; Baerends, E. J. *Comput. Phys. Commun.* **1999**, *118*, 119.
(11) Becke, A. D. *Phys. Rev. A* **1988**, *38*, 3098.
(12) Perdew, J. P. *Phys. Rev. A* **1986**, *33*, 8822.
(13) Dey, S.; Jain, V. K.; Knoedler, A.; Lissner, F.; Kaim, W. *J. Chem. Soc., Dalton Trans.* **2001**, 723.

**Scheme 1**

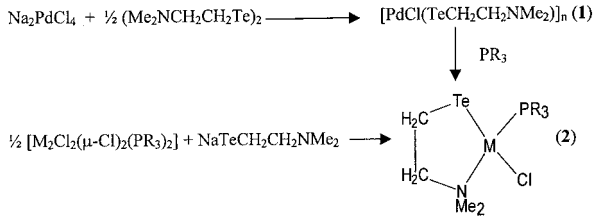


| M | $PR_3$ | |
|---|---|---|
| Pd | $PEt_3$ | **2a** |
| Pd | $PPr^n_3$ | **2b** |
| Pd | $PBu^n_3$ | **2c** |
| Pd | $PMe_2Ph$ | **2d** |
| Pd | $PMePh_2$ | **2e** |
| Pd | $PPh_3$ | **2f** |
| Pd | $PTol_3$ | **2g** |
| Pt | $PMe_2Ph$ | **2h** |
| Pt | $PMePh_2$ | **2i** |

**Table 2.** Selected Bond Distances (Å) and Bond Angles (deg) of $[MCl(ECH_2CH_2NMe_2)(PR_3)]$

| | M/E/$PR_3$ | | | |
|---|---|---|---|---|
| | Pd/Te/$PPr^n_3$ (**2b**) | Pd/Te/$PMePh_2$ (**2e**) | Pt/Te/$PMePh_2$ (**2i**) | Pt/Se/$PEt_3$ (**3**) |
| M−E | 2.5095(8) | 2.5156(6) | 2.5261(5) | 2.3563(10) |
| M−Cl | 2.3740(12) | 2.3929(14) | 2.3780(14) | 2.356(2) |
| M−P | 2.2295(11) | 2.2093(13) | 2.2189(12) | 2.210(2) |
| M−N | 2.172(3) | 2.143(4) | 2.182(4) | 2.160(7) |
| E−C(1) | 2.137(5) | 2.153(6) | 2.150(6) | 1.945(11) |
| N−C(3) | 1.457(5) | 1.409(6) | 1.447(6) | 1.456(16) |
| N−C(4) | 1.449(5) | 1.440(7) | 1.506(7) | 1.497(14) |
| N−C(2) | 1.509(6) | 1.481(7) | 1.467(7) | 1.476(12) |
| C(1)−C(2) | 1.453(7) | 1.439(8) | 1.474(10) | 1.483(16) |
| N−M−P | 179.19(8) | 178.89(13) | 178.69(11) | 175.9(4) |
| N−M−Cl | 91.89(9) | 94.07(13) | 91.58(11) | 92.6(2) |
| P−M−Cl | 88.62(4) | 86.84(5) | 87.52(5) | 87.12(10) |
| N−M−E | 87.85(9) | 86.61(13) | 87.32(11) | 86.3(2) |
| P−M−E | 91.59(3) | 92.56(4) | 93.66(4) | 93.86(7) |
| Cl−M−E | 176.22(3) | 173.20(4) | 175.16(3) | 177.57(11) |
| C(1)−E−M | 91.35(13) | 92.36(17) | 91.88(17) | 97.0(3) |
| C(3)−N−C(4) | 109.9(4) | 103.9(5) | 107.2(5) | 107.1(9) |
| C(3)−N−C(2) | 104.9(3) | 109.3(4) | 114.2(5) | 110.4(10) |
| C(4)−N−C(2) | 110.1(4) | 110.2(5) | 102.6(4) | 107.6(9) |
| C(3)−N−M | 111.2(3) | 109.2(3) | 108.6(3) | 107.0(7) |
| C(4)−N−M | 107.3(3) | 109.6(4) | 110.9(3) | 112.7(7) |
| C(2)−N−M | 113.5(3) | 114.2(4) | 113.0(3) | 111.9(6) |
| C(2)−C(1)−E | 109.2(3) | 106.9(4) | 108.5(4) | 108.6(6) |
| C(1)−C(2)−N | 114.9(4) | 116.7(4) | 116.3(5) | 113.7(9) |

P) for the platinum complexes suggests that the phosphine ligand is trans to the nitrogen atom of the chelating group,[4a,14,15] which is confirmed by X-ray structural analysis.

**Structures of Complexes 2b, 2e, 2i, and 3.** Crystallographic information on the four structurally characterized complexes is summarized in Table 1, and the bond parameters are given in Table 2. Compounds **2e** (Pd) and **2i** (Pt) are isostructural.

(14) Narayan, S.; Jain, V. K.; Varghese, B. *J. Chem. Soc., Dalton Trans.* **1998**, 2359.
(15) Jain, V. K.; Kannan, S.; Butcher, R. J.; Jasinski, J. P. *Polyhedron* **1995**, *14*, 3641.

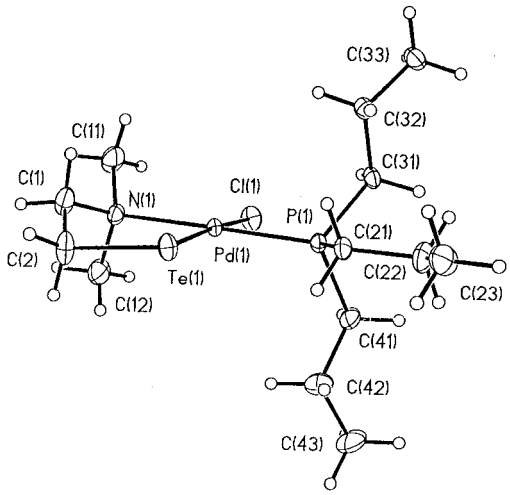


**Figure 1.** Molecular structure of $[PdCl(TeCH_2CH_2NMe_2)(PPr^n_3)]$ (**2b**) with crystallographic numbering scheme.

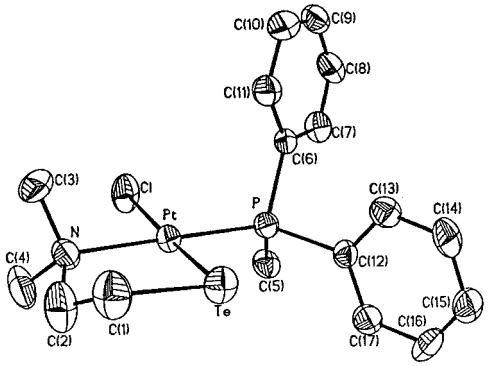


**Figure 2.** ORTEP plot $[PtCl(TeCH_2CH_2NMe_2)(PMePh_2)]$ (**2i**) with crystallographic numbering scheme.

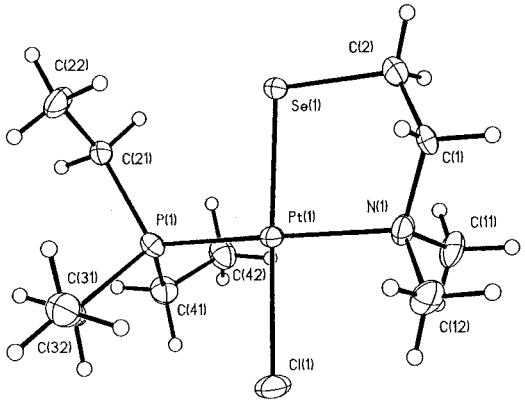


**Figure 3.** ORTEP plot $[PtCl(SeCH_2CH_2NMe_2)(PEt_3)]$ (**3**) with crystallographic numbering scheme.

Figures 1−3 illustrate a coordination arrangement in which an approximately square planar $M^{II}$ center is surrounded by Te (or Se), N, Cl, and P atoms with the neutral group 15 donor atoms in trans position to each other. Consequently, the charged donors (chloride and Te or Se) also adopt a mutual trans arrangement. The five-membered chelate rings exhibit a twist conformation with the carbon atoms lying on opposite sides of the metal coordination plane. With the unsymmetrical triorganophosphine $PMePh_2$ in **2e** and **2i** the P−C(phenyl) bonds to C(12) lie virtually in the best plane PtTeNClP (Figure 2). The bond lengths (M−Te,[16−18] Te−

**Table 3.** UV/Vis Absorption Data[a] of Complexes in $CH_2Cl_2$

| complex | $\lambda_{max}$ ($\epsilon$) |
|---|---|
| [PdCl($TeCH_2CH_2NMe_2$)($PEt_3$)] (**2a**) | 260 (27952), 288 (11050), 355(2500), 575 (140) |
| [PdCl($TeCH_2CH_2NMe_2$)($PPr^n_3$)] (**2b**) | 258 (34500), 288 (13970), 359(2700), 578 (290) |
| [PdCl($TeCH_2CH_2NMe_2$)($PBu^n_3$)] (**2c**) | 255 (27500), 287 (12000), 345 (2680), 573 (210) |
| [PdCl($TeCH_2CH_2NMe_2$)($PMe_2Ph$)] (**2d**) | 225 (21500), 262 (29000), 287 (12700), 358 (2700), 587 (180) |
| [PdCl($TeCH_2CH_2NMe_2$)($PMePh_2$)] (**2e**) | 223 (42180), 264 (41170), 359 (sh, 3570), 599 (280) |
| [PdCl($TeCH_2CH_2NMe_2$)($PPh_3$)] (**2f**) | 224 (32000), 269 (21650), 367 (sh), 623 (150) |
| [PdCl($TeCH_2CH_2NMe_2$){$PTol_3$}] (**2g**) | 240 (27400), 270 (sh), 349 (7542), 615 (141) |
| [PtCl($TeCH_2CH_2NMe_2$)($PMe_2Ph$)] (**2h**) | 241 (20700), 265 (sh), 295 (sh), 452 (150) |
| [PtCl($TeCH_2CH_2NMe_2$)($PMePh_2$)] (**2i**) | 243 (17200), 270 (sh), 300 (sh), 460 (140) |
| [PtCl($SeCH_2CH_2NMe_2$)($PEt_3$)] (**3**)[b] | 284, 405 |

[a] Wavelengths $\lambda_{max}$ at the absorption maxima in nm, molar extinction coefficients $\epsilon$ in $M^{-1}$ $cm^{-1}$. [b] From ref 4a.

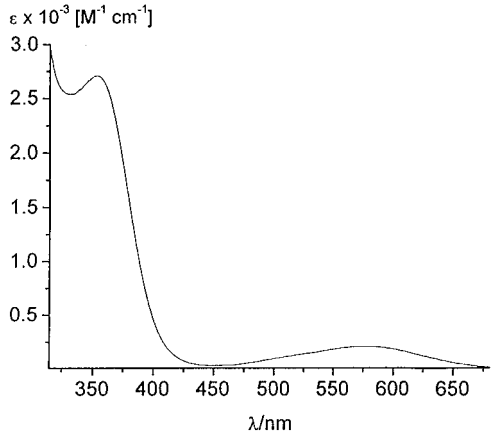


**Figure 4.** UV/vis spectrum of [PdCl($TeCH_2CH_2NMe_2$)($PPr^n_3$)] (**2b**) in $CH_2Cl_2$ solution.

$C$[16−19]) and bond angles are not unusual; obviously, the Pt−Te bond is longer in **2i** at 2.5261(5) Å than the Pt−Se bond at 2.3563(10) Å in **3** or 2.3773(7) Å in the directly related [PtCl($SeCH_2CH_2NMe_2$)($PMePh_2$)].[4a]

**UV/Vis Absorption Spectra.** All complexes described here are distinctly colored, either blue (Pd compounds) or red (Pt complexes). Well-separated, broad but relatively weak ($\epsilon \approx 200$ $M^{-1}$ $cm^{-1}$) bands in the visible are responsible for this color. Figure 4 shows a representative example, and Table 3 summarizes the absorption data in dichloromethane solution; studies in acetone solution for selected examples showed essentially similar absorption features within experimental uncertainty (±5 nm) of $\lambda_{max}$. In the series of palladium(II) complexes there is a clear trend for the long-wavelength band. Its wavelength at the absorption maximum decreases with increasing donor and decreasing acceptor strength of the triorganophosphine, i.e., in the series $PPh_3$ > $PMePh_2$ > $PMe_2Ph$ > $P(alkyl)_3$ (Table 3). The platinum(II) complexes have their absorptions at much higher energies, at about 460 nm (2.70 eV)[4a] as compared to about 600 nm (2.07 eV) for the palladium(II) analogues.

**Cyclic Voltammetry.** Although both the oxidation and the reduction of the complexes occur irreversibly, the comparison of electrochemical peak potentials can provide an estimate for the relative positioning of the frontier orbitals. Table 4 contains the relevant data for selected compounds.

**Table 4.** Electrochemical Data[a] of Complexes

| | | $E_{pa}$(ox) | $E_{pc}$(red) |
|---|---|---|---|
| [PdCl($TeCH_2CH_2NMe_2$)($PMePh_2$)][b] | (**2e**) | 0.25 | −2.12 |
| [PdCl($TeCH_2CH_2NMe_2$)($PPr^n_3$)][b] | (**2b**) | 0.27 | −2.35 |
| [PtCl($TeCH_2CH_2NMe_2$)($PMe_2Ph$)][b] | (**2h**) | 0.07 | *d* |
| [PtCl($TeCH_2CH_2NMe_2$)($PMe_2Ph$)][c] | (**2h**) | 0.01 | −2.68 |
| [PtCl($TeCH_2CH_2NMe_2$)($PMePh_2$)][b] | (**2i**) | 0.07 | *d* |
| [PtCl($TeCH_2CH_2NMe_2$)($PMePh_2$)][c] | (**2i**) | 0.03 | −2.63 |
| [PtCl($SeCH_2CH_2NMe_2$)($PMePh_2$)][b,e] | | 0.28 | *f* |
| [PtCl($SeCH_2CH_2NMe_2$)($PMe_2Ph$)][b,e] | | 0.34 | *f* |
| [PtCl($SeCH_2CH_2NMe_2$)($PEt_3$)][b] | (**3**) | 0.30 | *f* |
| [PdCl($SeCH_2CH_2NMe_2$)($PPh_3$)][b,e] | | 0.55 | −2.04 |

[a] Scan rate 100 mV/s, peak potentials for irreversible processes in V vs $FeCp_2/FeCp_2^+$. [b] Measurement in $CH_2Cl_2/Bu_4NPF_6$. [c] Measurement in DMF/$Bu_4NPF_6$. [d] Not applicable. [e] From ref 4a. [f] Not observed (<−2.7 V).

In the series of the complexes with $PMePh_2$ as a ligand, the rather facile oxidation occurs most easily for the "PtTe" complex **2i** whereas the "PdTe" system **2e** and the "PtSe" compound **3** exhibit slightly, about 0.2 V higher anodic peak potentials. A much stronger effect is apparent on the reductive side. Whereas the "PdTe" compound **2e** is reduced at a fairly negative but still well-accessible potential, the platinum complexes **2i** and **3** display a large negative potential shift >0.50 V relative to the Pd analogues. This effect is in agreement with the hypsochromic shift of the long-wavelength (HOMO−LUMO) transition when exchanging Pd by Pt.

**Calculations and Discussion of the Electronic Structure.** The DFT calculations essentially reproduce the experimental structures of the palladium and the platinum compounds (Table 5). The strongest discrepancies occur for the Te−C and M−X (X = Te, N) bonds which are calculated with too long distances by about 0.05 Å.

Based on either the calculated or the experimental geometries the DFT procedure yields MO situations where the highest occupied orbitals are centered on the tellurolate (with some metal contribution) whereas the lowest unoccupied MOs are identified as more mixed orbitals involving more (Pt) or less (Pd) contribution from the triorganophosphine ligand (Tables 6−8, Figure 5).

For instance, the ADF/BP calculated compositions of molecular orbitals of [PdCl($TeCH_2CH_2NMe_2$)($PMePh_2$)] (**2e**) are summarized in Table 6. The highest occupied molecular orbital (HOMO), 71a, is predominantly formed by Te p orbitals with contributing 4d orbitals of Pd. The Pd 4d and

(16) Jain, V. K.; Kannan, S.; Bohra, R. *Polyhedron* **1992**, *11*, 1551.
(17) Singh, A. K.; Srivastava, V.; Dhingra, S. K.; Drake, J. E.; Bailey, J. H. *Acta Crystallogr.* **1992**, *C48*, 655.
(18) Giolando, D. M.; Rauchfuss, T. B.; Rheingold, A. L. *Inorg. Chem.* **1987**, *26*, 1636.
(19) Drake, J. E.; Bailey, J. H. E.; Singh, A. K.; Srivastava, V. *Acta Crystallogr.* **1993**, *C49*, 684.

**Table 5.** Comparison of ADF/BP Calculated Bond Lengths and Angles with Experimental Data for [MCl(TeCH$_2$CH$_2$NMe$_2$)(L)] (L = PMePh$_2$, PPr$_3$)

| | Pd/Te/PMePh$_2$ (**2e**) | | Pd/Te/PPr$^n_3$ (**2b**) | | Pt/Te/PMePh$_2$ (**2i**) | |
|---|---|---|---|---|---|---|
| | calcd | exptl | calcd | exptl | calcd | exptl |
| M−Te | 2.567 | 2.516 | 2.580 | 2.510 | 2.585 | 2.526 |
| M−Cl | 2.399 | 2.393 | 2.401 | 2.374 | 2.409 | 2.378 |
| M−P | 2.232 | 2.209 | 2.247 | 2.230 | 2.222 | 2.219 |
| M−N | 2.205 | 2.143 | 2.213 | 2.172 | 2.206 | 2.182 |
| Te−C(1) | 2.199 | 2.153 | 2.192 | 2.137 | 2.196 | 2.150 |
| N−M−P | 179.0 | 178.9 | 179.1 | 179.2 | 177.8 | 178.7 |
| N−M−Cl | 92.5 | 94.1 | 91.9 | 91.9 | 90.8 | 91.6 |
| P−M−Cl | 86.7 | 86.8 | 87.4 | 88.6 | 87.6 | 87.5 |
| N−M−Te | 88.6 | 86.6 | 87.7 | 87.9 | 87.9 | 87.3 |
| P−M−Te | 92.1 | 92.6 | 93.0 | 91.6 | 93.6 | 93.7 |
| C(1)−Te−M | 90.1 | 92.4 | 90.0 | 91.4 | 90.6 | 91.9 |
| C(2)−N−M | 113.1 | 114.2 | 114.4 | 113.5 | 113.5 | 113.0 |

**Table 6.** ADF/BP Calculated One-Electron Energies and Percentage Composition of Selected Highest Occupied and Lowest Unoccupied Molecular Orbitals of [PdCl(TeCH$_2$CH$_2$NMe$_2$)(PMePh$_2$)] (**2e**) Expressed in Terms of Composing Fragments

| MO | *E* (eV) | prevailing character | Pd | PMePh$_2$ | Te | Cl | N |
|---|---|---|---|---|---|---|---|
| unoccupied | | | | | | | |
| 74a | −1.98 | PMePh$_2$ | 3 (d) | 90 | 2 | 2 | |
| 73a | −2.08 | PMePh$_2$ | 2 (d) | 94 | | | |
| 72a | −2.70 | $d_{Pd}$ + PMePh$_2$ + Te | 24 (d) | 39 | 25 | 8 | 3 |
| occupied | | | | | | | |
| 71a | −4.31 | Te + $d_{Pd}$ | 18 (d) | | 70 | 9 | |
| 70a | −5.46 | $d_{Pd}$ | 11 (s); 63 (d) | 4 | 12 | 14 | 2 |
| 69a | −5.58 | Cl + $d_{Pd}$ | 20 (d) | 3 | | 68 | |
| 68a | −5.65 | Cl + $d_{Pd}$ | 2 (s); 2 (p); 22 (d) | 3 | 13 | 49 | |
| 67a | −5.91 | Cl + Te | 3 (p); 11 (d) | 2 | 41 | 38 | |
| 66a | −6.38 | $d_{Pd}$ | 83 (d) | 10 | 1 | 1 | |
| 65a | −6.60 | PMePh$_2$ | 18 (d) | 62 | 4 | 6 | 7 |

**Table 7.** ADF/BP Calculated One-Electron Energies and Percentage Composition of Selected Highest Occupied and Lowest Unoccupied Molecular Orbitals of [PdCl(TeCH$_2$CH$_2$NMe$_2$)(PPr$^n_3$)] (**2b**) Expressed in Terms of Composing Fragments

| MO | *E* (eV) | prevailing character | Pd | PPr$^n_3$ | Te | Cl | N |
|---|---|---|---|---|---|---|---|
| unoccupied | | | | | | | |
| 70a | −0.13 | PPr$^n_3$ + $d_{Pd}$ | 34 (d) | 60 | 3 | 1 | |
| 69a | −0.44 | Te | 13 (d) | 7 | 54 | | 1 |
| 68a | −2.10 | $d_{Pd}$ + PPr$^n_3$ + Te | 30 (d) | 20 | 29 | 10 | 6 |
| occupied | | | | | | | |
| 67a | −4.11 | Te + $d_{Pd}$ | 20 (d) | 3 | 68 | 8 | |
| 66a | −5.24 | $d_{Pd}$ | 12 (s); 63 (d) | 3 | 11 | 4 | 1 |
| 65a | −5.39 | Cl + $d_{Pd}$ | 24 (d) | 3 | | 66 | |
| 64a | −5.53 | Cl + $d_{Pd}$ | 25 (d) | | 18 | 51 | |
| 63a | −5.77 | Cl + Te | 4 (p); 7 (d) | 1 | 43 | 37 | |
| 62a | −6.11 | $d_{Pd}$ | 87 (d) | 8 | 1 | 1 | |
| 61a | −6.78 | | 18 (d) | 62 | 4 | 6 | 7 |

Cl 3p orbitals contribute significantly to the next lower lying occupied MOs 68a−70a. The lowest lying unoccupied molecular orbital (LUMO) is delocalized over the system with a large contribution from PMePh$_2$ (39%). Several higher lying unoccupied orbitals are present which largely involve the phenyl groups of the PMePh$_2$ fragment, an effect which is absent in the otherwise similar trialkylphosphine system **2b** (Table 7). Table 8 compares the energies and compositions of frontier molecular orbitals within the structurally characterized series of [MCl(TeCH$_2$CH$_2$NMe$_2$)(L)] complexes. Figure 5 shows the LUMO composition of the Pd/Te/PPr$^n_3$ complex **2b**. Variation of the central metal or L affects mainly the composition of the LUMO, where the L contribution varies from 20% to 60% on going from the Pd/Te/PPr$^n_3$ system (**2b**) to the Pt/Te/PMePh$_2$ complex **2i**. The composition of the set of highest occupied orbitals is only moderately influenced.

**Table 8.** ADF/BP Calculated One-Electron Energies and Percentage Composition of Frontier Molecular Orbitals of [MCl(TeCH$_2$CH$_2$NMe$_2$)(L)] Complexes Expressed in Terms of Composing Fragments

| complex | MO | *E* (eV) | prevailing character | M | L | Te | Cl | N |
|---|---|---|---|---|---|---|---|---|
| Pd/Te/PMePh$_2$ (**2e**) | LUMO (72a) | −2.70 | $d_{Pd}$ + PMePh$_2$ + Te | 24 | 39 | 25 | 8 | 3 |
| | HOMO (71a) | −4.31 | Te + $d_{Pd}$ | 18 | | 70 | 9 | |
| Pt/Te/PMePh$_2$ (**2i**) | LUMO (79a) | −2.27 | $d_{Pt}$ + PMePh$_2$ + Te | 18 | 60 | 10 | 4 | 2 |
| | HOMO (78a) | −4.09 | Te + $d_{Pt}$ | 23 | | 66 | 7 | |
| Pd/Te/PPr$^n_3$ (**2b**) | LUMO (68a) | −2.10 | $d_{Pd}$ + PPr$^n_3$ + Te | 30 | 20 | 29 | 10 | 6 |
| | HOMO (67a) | −4.11 | Te + $d_{Pd}$ | 20 | 3 | 68 | 8 | |

**Table 9.** Selected ADF/BP Calculated Lowest Singlet Excitation Energies for [PdCl(TeCH$_2$CH$_2$NMe$_2$)(PPr$^n_3$)] (**2b**; $^1A_1$ States)

| main character (% composition) | excn energy (eV) | oscillator strength |
|---|---|---|
| 99 (67a → 68a) (HOMO → LUMO) | 1.98 | 0.0004 |
| 93 (66a → 68a) | 3.15 | 0.006 |
| 95 (65a → 68a) | 3.20 | 0.002 |
| 97 (67a → 69a) | 3.65 | 0.002 |
| 60 (67a → 70a); 37 (63a → 68a) | 3.84 | 0.019 |
| 95 (65a → 68a | 4.03 | 0.015 |
| 35 (63a → 68a); 29 (67a → 70a); 14 (61a → 68a); 6 (60a → 68a) | 4.27 | 0.140 |

These calculated variations of the HOMO/LUMO positions in Table 8 confirm the shifts of redox potentials within this series of complexes. Specifically, the changes within the isostructural series **2e**/**2i**, viz., $E_{LUMO}$(**2i**) − $E_{LUMO}$(**2e**) = 0.43 eV and $E_{HOMO}$(**2i**) − $E_{HOMO}$(**2e**) = 0.22 eV, show broad agreement with the experimental peak potential differences $E_{pc}$(**2e**) − $E_{pc}$(**2i**) = 0.51 V and $E_{pa}$(**2e**) − $E_{pa}$(**2i**) = 0.18 V (Table 4).

The TD-DFT calculated lowest excitation energies for [PdCl(TeCH$_2$CH$_2$NMe$_2$)(PPr$^n_3$)] (**2b**) are listed in Table 9. Calculations for the PMe$_2$Ph- and PMePh$_2$-containing systems **2e** and **2i** produced many additional weak low-energy transitions to unoccupied orbitals involving the phenyl groups; we therefore restrict the discussion largely to that of the trialkylphosphine−palladium complex **2b** and its calculated platinum analogue. In all cases, the lowest calculated excitation corresponds to a transition from the largely Te based HOMO into a more delocalized LUMO with significant Te, metal, phosphine, and even some chloride contributions. Although pure ligand-field (d−d) transitions would also result in weak, broad absorptions, the remaining empty metal d orbital of the d$^8$ system is too high in energy to be involved in low-energy transitions.

According to Tables 8 and 9, the low-energy electronic transitions responsible for the colors can thus be described mainly as ligand(Te)-to-ligand(PR$_3$) charge transfer transitions in the case of Pt complexes whereas the target MO is of more mixed character for the Pd analogues with their

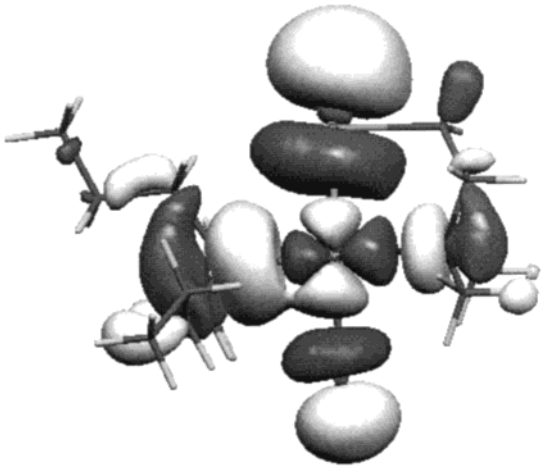

**Figure 5.** LUMO representation of [PdCl($TeCH_2CH_2NMe_2$)($PPr^n_3$)] (**2b**). Donor atoms around $Pd^{II}$: Te, N, Cl, P (clockwise, starting from the top).

unusually low transition energies. The calculated value of 1.98 eV (626 nm) for **2b** is in reasonable agreement with the experimental absorption maximum at 2.14 eV (578 nm, Table 3). The low intensity of this long-wavelength transition is well reproduced by the TD-DFT procedure; the next transitions for **2b** (Table 9) which are well separated from the HOMO−LUMO transition both experimentally (Figure 5, Table 3) and from the DFT calculation (Table 9) can be characterized as excitations from Pd- or Cl-localized orbitals into the L-localized LUMOs. The TD-DFT calculated lowest transitions for Pd/Te/$PMePh_2$ (**2e**), Pd/Te/$PMe_2Ph$ (**2d**), and Pd/Te/$PPr^n_3$ (**2b**) are 1.77, 1.93, and 1.98 eV, respectively. Calculated values for Pt/Te/$PMePh_2$ (**2i**), Pt/Te/$PMe_2Ph$ (**2b**), and Pt/Te/$PPr^n_3$ are 1.88, 2.07, and 2.37 eV, respectively. These calculated trends are in agreement with the experimental variations of the lowest transitions resulting from $PR_3$ ligand changes within both series of M/Te/$PR_3$ complexes. The shift of the lowest transition to higher energies on replacement of Pd by Pt for individual members of the series is underestimated but qualitatively reproduced.

Summarizing, we have used both experiments and DFT calculations for mixed-ligand complexes of $Pd^{II}$ and $Pt^{II}$ to establish the nature of the remarkably low energy charge transfer transitions from the p(Te) HOMO to unoccupied orbitals of more (Pd) or less (Pt) mixed character with large $PR_3$ contributions. Due to the involvement of heavier elements in the frontier orbitals we have validated the DFT results through crystallographic confirmation of structure calculations and through studies of the spectroscopic and electrochemical response on variation of the organophosphine acceptor ligands. In chemical terms, the stronger back-bonding interaction between $Pt^{II}$ vs $Pd^{II}$ and the phosphine acceptors destabilizes the LUMO (more negative reduction potential) whereas the replacement of Se by Te causes the expected destabilization of the HOMO (lower oxidation peak potential). The variation of the phosphines confirms that the LUMO is indeed an orbital with considerable $PR_3$ contributions; the lower lying unoccupied orbitals of the aromatic derivatives cause the bathochromic shift observed in Table 3. It is confirmed[1] that the electronically rather inert $Pd^{II}$ and $Pt^{II}$ centers are particularly suitable to allow observation of ligand−ligand charge transfer processes, even with less common combinations of donor and acceptor groups.

**Acknowledgment.** We thank Drs. J. P. Mittal and P. Raj for encouragement of this work. We are grateful to Dr. P. K. Mathur, Head, Analytical Chemistry Division BARC, for providing microanalysis of the compounds. Support of this work from BMBF (Project No. IND 99/060), the DFG, FCI, the Ministry of Education of the Czech Republic, and the DLR (Bonn) for KONTAKT Project CZE 00/013 is gratefully acknowledged.

**Supporting Information Available:** Details of the X-ray structure determination (four compounds) in CIF format. This material is available free of charge via the Internet at http://pubs.acs.org.

IC011210V